Inverse Monte Carlo determination of effective lattice models for $SU(3)$ Yang-Mills theory at finite temperature

Christian Wozar, Tobias Kaestner, and Andreas Wipf

Theoretisch-Physikalisches Institut, Friedrich-Schiller-Universität Jena, Max-Wien-Platz 1, 07743 Jena, Germany

Thomas Heinzl

School of Mathematics and Statistics, University of Plymouth, Drake Circus, Plymouth, PL4 8AA, United Kingdom
(Received 27 April 2007; published 4 October 2007)

This paper concludes our efforts in describing $SU(3)$-Yang-Mills theories at different couplings/ temperatures in terms of effective Polyakov-loop models. The associated effective couplings are determined through an inverse Monte Carlo procedure based on novel Schwinger-Dyson equations that employ the symmetries of the Haar measure. Because of the first-order nature of the phase transition we encounter a fine-tuning problem in reproducing the correct behavior of the Polyakov-loop from the effective models. The problem remains under control as long as the number of effective couplings is sufficiently small.

I. INTRODUCTION

Since the pioneering papers of Polyakov [1] and Susskind [2] the confinement-deconfinement phase transition in finite-temperature Yang-Mills theory has become a thoroughly studied phenomenon. This is particularly true for the "standard" groups $SU(2)$ and $SU(3)$, but more "exotic" groups like $G(2)$ have recently come into focus as well, see e.g. [3,4]. Because of the nonperturbative nature of the problem progress has mainly been achieved via brute force lattice computations.

Nevertheless, it would be helpful to have a simpler and more intuitive understanding of the physics involved. The principal tool for this purpose is the construction and subsequent analysis of effective models. Such attempts also have quite some history going back to the works of Svetitsky and Yaffe [5,6] as well as Polonyi and Szlachanyi [7]. The basic idea (in the spirit of Landau and Ginzburg) is to use the order parameter of the transition, the Polyakov loop, as a collective degree of freedom and formulate effective theories in terms of it. For gauge groups $SU(N)$ the rationale behind that is the Svetitsky-Yaffe conjecture [5,6] which states that the Yang-Mills finite-temperature transition in dimension $d + 1$ is described by an effective spin model in d dimensions with short-range interactions.[1] These ideas have initially been taken up in terms of strong-coupling expansions [7,9,10] yielding Ising type spin models with an effective coupling $\lambda(\beta)$ where β denotes the Yang-Mills-Wilson coupling. A review of early work in this context may be found in [11]. For an overview of more recent developments we refer the reader to [12].

Early on, it has also been attempted to obtain these effective models, that is their couplings (being the "weights" of the included operators) nonperturbatively via lattice methods. In [13,14] Creutz's microcanonical demon method [15] has been employed for $SU(2)$. An alternative method based on Schwinger-Dyson equations (SDEs) and dubbed "inverse Monte Carlo" (IMC) was developed soon after [16,17] and applied to both $SU(2)$ [18,19] and $SU(3)$ [20,21]. Since then the IMC approach to lattice gauge theories has largely been dormant with only a few exceptions [22,23].

Inspired by the success of Polyakov-loop models [24–26] we have recently reinvestigated the feasibility of IMC for the confinement-deconfinement phase transition in a series of papers. Our numerical approach has consistently been complemented by analytical attempts such as strong-coupling expansions and mean-field approximations. For the second-order $SU(2)$ transition our results may be found in [27,28]. By including up to 14 operators and 3 different group representations we were able to reproduce suitable Yang-Mills observables to a reasonable accuracy. The same is true for the analytically known asymptotic behavior of the effective couplings as a function of β. In [29] we have started to investigate effective models for $SU(3)$ which are generalizations of the 3-states Potts model. The critical behavior of these is an interesting subject in its own right. We have found a very rich phase structure with first and second-order transitions between symmetric, ferromagnetic, and antiferromagnetic phases. In addition there seems to be a tricritical point rendering mean-field theory approximately exact in its vicinity .

In relating the effective models to $SU(3)$ Yang-Mills via IMC one expects to encounter new difficulties. The first technical problem to overcome is to find the SDEs which are less straightforward than for $SU(2)$ as the $SU(3)$ group manifold no longer is a sphere. This problem has been solved in [31,32]. As the $SU(3)$ phase transition is of (weak) first order, hence not continuous, the determination of the effective couplings might require fine-tuning raising

---

[1]The reasoning involved strongly relies on center symmetry. The study of more exotic Lie groups (which may not even have a nontrivial center) suggests that the size of the gauge group is also important [8].

the question of stability of the solutions. This will be one of the main issues to be addressed in what follows.

The remainder of the paper is organized as follows. In Sec. II we suggest different effective actions as candidates for describing the Polyakov-loop dynamics of Yang-Mills theory. In Sec. III we explain how to obtain the effective couplings via two alternative sets of SDEs and subsequent IMC. Our numerical results are presented in Sec. IV. Section V concludes our discussion with a summary and outlook. Some technicalities are deferred to Appendices A, B, and C.

II. EFFECTIVE ACTIONS

We begin by recalling the lattice definition of the untraced Polyakov loop in the group representation $\mathcal{R}$,

$$\mathcal{R}(\mathfrak{P}_x) \equiv \prod_{t=1}^{N_t} \mathcal{R}(U_{tx}), \qquad (1)$$

where $\mathcal{R}(U_{tx})$ is the temporal link at time slice t and position x in representation $\mathcal{R}$. Any irreducible representation of $SU(3)$ is labeled by two integers, $\mathcal{R} = \mathcal{R}_{pq}$, which, in flavor language, count the number of quarks and antiquarks needed to construct the multiplet associated with $\mathcal{R}_{pq}$. The basic building blocks of our effective actions are the group characters $\chi_{\mathcal{R}}$ associated with the representation $\mathcal{R}$, that is the traces of the Polyakov loop (1),

$$\chi_{\mathcal{R}}(\mathcal{P}) \equiv \chi_{pq}(\mathcal{P}) \equiv \operatorname{tr} \mathcal{R}_{pq}(\mathfrak{P}). \qquad (2)$$

Note that these only depend on the traced Polyakov loop in the fundamental representation, $\mathcal{P} = \operatorname{tr} \mathfrak{P}$. The trivial character is of course $\chi_{00} = 1$ while the first nontrivial ones correspond to the (anti-)fundamental representations and yield just the standard traced Polyakov loop (and its complex conjugate),

$$\chi_{10}(\mathcal{P}) = \mathcal{P}, \qquad \chi_{01}(\mathcal{P}) = \mathcal{P}^*. \qquad (3)$$

Under a center transformation, the characters transform as

$$\chi_{pq} \to z^{p-q} \chi_{pq}, \qquad z \in \mathbb{Z}_3. \qquad (4)$$

Center symmetry is then sufficient to determine the operator content of the effective action if we restrict to nearest-neighbor (NN) interactions. In terms of group characters one finds the general form

$$S_{\text{eff}}[\chi] = \sum_{\substack{\langle xy \rangle, pq, p'q' \\ p+p'=q+q' \bmod 3}} \lambda_{pq,p'q'} \chi_{pq}(\mathcal{P}_x) \chi_{p'q'}(\mathcal{P}_y), \qquad (5)$$

where the sum over representations is constrained by center symmetry. Expressing the characters explicitly in terms of the Polyakov loop $\mathcal{P}$ one easily recognizes (5) as the action suggested by Dumitru *et al.* [24]. Their "potential terms," built from single center symmetric characters located at single sites appear whenever the second adjacent

character is trivial, $\chi_{00} = 1$. In this case the typical hopping terms connecting NN sites "degenerate" into ultralocal terms, the one of lowest dimension being the "octet loop" contribution, $\lambda_{11,00}\chi_{11}$ as indeed $1 + 0 = 1 + 0 \bmod 3$. One expects that the couplings $\lambda_{pq,p'q'}$ decrease with increasing representation labels, p, q, p', and q', hence that representations of low dimension,

$$d_{pq} = \tfrac{1}{2}(p + 1)(q + 1)(p + q + 2), \qquad (6)$$

dominate the effective action. To simplify our notation we will henceforth write the action (5) (and generalizations thereof) as a series of the form

$$S_{\text{eff}} = \sum_i \lambda_i S_i, \qquad (7)$$

where up to 16 different terms S_i will be taken into consideration, albeit not necessarily within one and the same *ansatz*. A list of the operators S_i may be found in Appendix A where we allow for next-to-NN (NNN) couplings in addition. It is easy to check that each of the terms given satisfies the selection rules for the representation labels necessary for center symmetry.

It turns out (in hindsight) that the *ansätze* (5) or (7) contain more freedom of choice than actually required which makes the inverse Monte Carlo routines less efficient (see below). To further constrain this freedom we generalize to $SU(3)$ the strong-coupling approach introduced by Billo *et al.* [33] which we already have successfully applied to $SU(2)$ [28]. The basic building blocks are then given by the center symmetric operators connecting NN sites,

$$S_{\mathcal{R},\ell} \equiv \chi_{\mathcal{R}}(\mathcal{P}_x)\chi_{\mathcal{R}}^*(\mathcal{P}_y) + \text{c.c.}, \qquad \ell \equiv \langle xy \rangle. \qquad (8)$$

The strong-coupling expansion then replaces the *ansatz* (5) by the following somewhat more complicated expression [31],

$$S_{\text{eff}} = \sum_r \sum_{\mathcal{R}_1 \dots \mathcal{R}_r} \sum_{\ell_1 \dots \ell_r} c_{\mathcal{R}_1 \dots \mathcal{R}_r}^{\ell_1 \dots \ell_r}(\beta) \prod_{i=1}^r S_{\mathcal{R}_i,\ell_i}, \qquad (9)$$

where r counts the number of link operators (8) contributing at each order. The coefficients $c_{\mathcal{R}_1 \dots \mathcal{R}_r}^{\ell_1 \dots \ell_r}$ are the couplings between the operators $S_{\mathcal{R}_i,\ell_i}$ from (8) sitting at NN links $\ell_i \equiv \langle x_i, y_i \rangle$ in representation $\mathcal{R}_i$. The effective action defined in (9) hence describes a network of link operators of the type (8) that are collected into (possibly disconnected) "polymers" contributing with "weight" $c_{\mathcal{R}_1 \dots \mathcal{R}_r}^{\ell_1 \dots \ell_r}$. Again, one expects the "weights" or couplings to decrease as the dimensions of the representations and the interlink distances involved increase. In a strong-coupling (small-β) expansion truncated at $\mathcal{O}(\beta^{kN_t})$ one has $r \le k$ and the additional restriction $|\mathcal{R}_1| + \dots + |\mathcal{R}_r| < k$ with $|\mathcal{R}| \equiv p + q$ for a given representation $\mathcal{R}$.

To lowest order β^{N_t} one finds the universal effective action [7]

$$S_{\text{eff}} = c_{10} \sum_{\langle xy \rangle} S_{10,\langle xy \rangle} \equiv \kappa_1 \sum_{\langle xy \rangle} (\chi_{10}(\mathcal{P}_x)\chi_{01}(\mathcal{P}_y) + \text{c.c.})$$

$$\equiv \kappa_1 \sum_{\langle xy \rangle} (\mathcal{P}_x \mathcal{P}_y^* + \mathcal{P}_x^* \mathcal{P}_y), \tag{10}$$

which is just a single hopping term connecting Polyakov loops at NN sites. This is reminiscent of a generalized Ising model or, more appropriately, a three-state Potts model [34]. As mentioned before the study of these models is interesting in its own right [29] but will not be the topic of the present paper which focuses on the relation between the effective actions and Yang-Mills theory.

Again, the most general representation (9) is not too illuminating and we will therefore adopt the notation

$$S_{\text{eff}} = \sum_a \kappa_a I_a. \tag{11}$$

A list of the leading NN and NNN action terms I_a can be found in Appendix B.

In principle, without any truncations, the effective actions (7) and (11) have to coincide although the operator bases used are different. Accordingly, there is a linear relationship between the couplings λ_i and κ_a. However, as the ordering principles for the two *ansätze* are not the same the relation between the couplings *after* truncation is *not* one-to-one but rather of the form

$$\lambda_i = K_{ia}\kappa_a. \tag{12}$$

Typically, for a given truncation of the λ-action (7) the range of the index i is larger than that of a, i.e. there are more λ's than κ's. Accordingly, the matrices (K_{ia}) are rectangular with $a < i$ and integer entries. For this reason it is calculationally often more efficient to work with the κ-action (11) and reobtain the λ_i via (12). Our standard choices for the numerical matrices (K_{ia}) corresponding to different truncations of the effective actions may be found in Appendix C. As the operators S_i appearing in (7) are more intuitive and resemble generalized spin terms we have decided, for the sake of brevity, to present results only for the λ's in this paper.

III. SCHWINGER-DYSON EQUATIONS AND INVERSE MONTE CARLO

In this section we shortly recapitulate the $SU(3)$ Schwinger-Dyson equations (SDEs) that have recently been derived in [31,32]. They will be the main tool to relate the effective actions (7) and (11) to Yang-Mills theory. Our numerical approach benefits from the fact that there are two independent versions of SDEs which in the end, however, should yield equivalent results. The first type of equations is based on an integral identity which is more algebraic in nature than the second type which follows from geometrical considerations.

A. Algebraic SDEs

It is useful to parametrize the diagonalized, untraced Polyakov loop by means of two angular variables, ϕ_1 and ϕ_2,

$$\mathfrak{P}(\phi_1, \phi_2) = \begin{pmatrix} e^{i\phi_1} & 0 & 0 \\ 0 & e^{i\phi_2} & 0 \\ 0 & 0 & e^{-i(\phi_1+\phi_2)} \end{pmatrix}, \tag{13}$$

with values in a fundamental region given by the restrictions

$$\phi_1 \le \phi_2 \le (-\phi_1 - \phi_2) \bmod 2\pi, \qquad 0 \le \phi_i < 2\pi. \tag{14}$$

As a result, the reduced Haar measure acquires the form

$$d\mu_{\text{red}} = J^2 d\phi_1 d\phi_2 \tag{15}$$

with a nontrivial Jacobian that may either be expressed in terms of characters,

$$J^2 = 15 - 6\chi_{11} + 3\chi_{30} + 3\chi_{03} - \chi_{22}, \tag{16}$$

or in terms of the trace $\mathcal{P}$ of (13),

$$J^2 = 27 - 18\mathcal{P}\mathcal{P}^* + 4\mathcal{P}^3 + 4\mathcal{P}^{*3} - \mathcal{P}^2\mathcal{P}^{*2}. \tag{17}$$

Using the latter variable leads to the remarkable algebraic identity

$$d\mu_{\text{red}}(\phi_1, \phi_2) = J^2 d\phi_1 d\phi_2 = J d\mathcal{P} d\mathcal{P}^*$$

$$= d\mu_{\text{red}}(\mathcal{P}, \mathcal{P}^*), \tag{18}$$

such that one can trade J^2 for its square root J. It is a fact of life that any function $f = f(\mathcal{P}, \mathcal{P}^*)$ vanishing on the boundary $\partial\Omega$ of a region Ω satisfies the integral identity

$$\int_\Omega d\mathcal{P} d\mathcal{P}^* \partial_{\mathcal{P}} f = 0, \tag{19}$$

which is reminiscent of integration by parts on the real line, $\int dx f'(x) = 0$ (for functions f vanishing at infinity). For our purposes we make the particular choice

$$f(\mathcal{P}, \mathcal{P}^*) = J^3 g(\mathcal{P}, \mathcal{P}^*) \tag{20}$$

with arbitrary g and integrate over the domain of $\mathcal{P}$ given implicitly via (14). This is consistent with the general identity (19) as the reduced Haar measure vanishes at the boundary $\partial\Omega$ of the fundamental region (14). Hence, (19) specializes to

$$0 = \int d\mu_{\text{red}}(\mathcal{P}_z, \mathcal{P}_z^*)\left(\frac{3}{2}\frac{\partial J_z^2}{\partial \mathcal{P}_z}g + J_z^2\frac{\partial g}{\partial \mathcal{P}_z}\right), \tag{21}$$

where we have used the reduced Haar measure from (18) and reinstated the dependence on the lattice site chosen to be z. The derivative of J^2 can actually be worked out with the result

$$\frac{\partial J^2}{\partial \mathcal{P}} = 12\mathcal{P}^2 - 2\mathcal{P}\mathcal{P}^{*2} - 18\mathcal{P}^*. \qquad (22)$$

To actually obtain genuine SDEs we have to introduce the usual Boltzmann factor $\exp(-S_{\text{eff}})$. This is done by choosing a special function g, namely

$$g_{\boldsymbol{x}} \equiv \frac{\partial h}{\partial \mathcal{P}_{\boldsymbol{x}}^*} \exp(-S_{\text{eff}}), \qquad (23)$$

with another function $h(\mathcal{P}, \mathcal{P}^*)$ required to be $\mathbb{Z}_3$ invariant,

$$h(\mathcal{P}, \mathcal{P}^*) = h(z\mathcal{P}, z^*\mathcal{P}^*), \qquad z \in \mathbb{Z}_3. \qquad (24)$$

Plugging in the *ansatz* (7) for the λ-action the $\mathcal{P}$-derivative of (23) needed for (21) becomes

$$\frac{\partial g_{\boldsymbol{x}}}{\partial \mathcal{P}_{\boldsymbol{z}}} = \left(h_{,\mathcal{P}_{\boldsymbol{x}}^*, \mathcal{P}_{\boldsymbol{z}}} - \sum_i \lambda_i h_{,\mathcal{P}_{\boldsymbol{x}}^*} S_{i, \mathcal{P}_{\boldsymbol{z}}} \right) e^{-S_{\text{eff}}}, \qquad (25)$$

where the commas denote differentiation with respect to the subsequent argument. Functional integration of (21) with the measure $\mathcal{D}\mu_{\text{red}} \equiv \prod_{\boldsymbol{z}} d\mu_{\text{red}}(\mathcal{P}_{\boldsymbol{z}}, \mathcal{P}_{\boldsymbol{z}}^*)$ finally yields the desired SDEs,

$$0 = \left\langle \frac{3}{2} \frac{\partial J_{\boldsymbol{z}}^2}{\partial \mathcal{P}_{\boldsymbol{z}}} h_{,\mathcal{P}_{\boldsymbol{x}}^*} + J_{\boldsymbol{z}}^2 h_{,\mathcal{P}_{\boldsymbol{x}}^*, \mathcal{P}_{\boldsymbol{z}}} \right\rangle - \sum_i \lambda_i \langle J_{\boldsymbol{z}}^2 h_{,\mathcal{P}_{\boldsymbol{x}}^*} S_{i, \mathcal{P}_{\boldsymbol{z}}} \rangle, \qquad (26)$$

which comprise a linear system for the effective couplings λ_i, generalizing analogous results for $SU(2)$ [27,28]. The experience gained there prompts us to choose the function h from the operators S_i in the *ansatz* for the λ-action (7). Any index i then yields an independent equation. In addition, this choice automatically satisfies the criterion (24) of $\mathbb{Z}_3$ invariance.

On top of that we will vary the sites $\boldsymbol{x}$ and $\boldsymbol{z}$, in particular, the distance $d \equiv |\boldsymbol{x} - \boldsymbol{z}|$ between them. On a lattice with spatial extent N_s this implies a range of distances $d \in \{0, \ldots, \lfloor N_s/2 \rfloor\}$ where $\lfloor x \rfloor$ denotes the largest integer $\leq x$. For N different operators S_i we thus obtain N independent equations for each distance d.

B. Geometrical SDEs

For any function $f = f(U)$ on a Lie group we define its left derivative in the direction of the generator T^a via

$$L_a f(U) \equiv \frac{d}{dt} f(e^{tT^a} U)\big|_{t=0}. \qquad (27)$$

Left invariance of the Haar measure implies a symmetry relation somewhat analogous to (19),

$$\int d\mu_{\text{Haar}}(U) L_a f(U) = 0, \qquad (28)$$

which will serve as a master identity generating all SDEs. As in the previous subsection we would like to integrate over the reduced Haar measure $d\mu_{\text{red}}$ only. Thus, we want the integrand $L_a f(U)$ to be a *class* function. If G is such a

class function it only depends on the fundamental group characters, $\chi_F(U) \equiv \text{tr}(\mathcal{R}_F(U))$, where $\mathcal{R}_F(U)$ denotes a fundamental representation of the group element U, i.e. **3** or $\bar{\textbf{3}}$ for $SU(3)$. For the particular choice $f = g L_a \chi_p$, with g an arbitrary class function and χ_p a fundamental character, the integrand in (28) indeed becomes a class function so that we end up with the "reduced" integral

$$\int d\mu_{\text{red}} L_a(g L^a \chi_p) = 0. \qquad (29)$$

For $SU(3)$ we obviously choose the fundamental character χ_p as the trace of the Polyakov loop in the fundamental representation, $\chi_p \equiv \chi_{10} \equiv \mathcal{P}$ and $g \equiv h e^{-S_{\text{eff}}}$, slightly different from (23). The left derivatives are worked out as follows [31,32],

$$L_a(L^a(\mathcal{P})) = -\tfrac{16}{3}\mathcal{P}, \qquad L_a(\mathcal{P})L^a(\mathcal{P}) = 4\mathcal{P}^* - \tfrac{4}{3}\mathcal{P}^2,$$
$$L_a(\mathcal{P})L^a(\mathcal{P}^*) = 6 - \tfrac{2}{3}|\mathcal{P}|^2, \qquad (30)$$

and only depend on the traced Polyakov loop as they should. Finally, to obtain feasible equations we choose h among the $\mathcal{P}$-derivatives of the S_i, $h = S_{i,\mathcal{P}_{\boldsymbol{x}}}$ implying the following set of geometrical SDEs,

$$0 = \left\langle -\frac{16}{3}\mathcal{P}_{\boldsymbol{z}} S_{i,\mathcal{P}_{\boldsymbol{x}}} + \left(4\mathcal{P}_{\boldsymbol{z}}^* - \frac{4}{3}\mathcal{P}_{\boldsymbol{z}}^2\right) S_{i,\mathcal{P}_{\boldsymbol{x}},\mathcal{P}_{\boldsymbol{z}}} \right.$$
$$+ \left(6 - \frac{2}{3}|\mathcal{P}_{\boldsymbol{z}}|^2\right) S_{i,\mathcal{P}_{\boldsymbol{x}},\mathcal{P}_{\boldsymbol{z}}^*} \right\rangle - \sum_j \lambda_j \left\langle \left(4\mathcal{P}_{\boldsymbol{z}}^* - \frac{4}{3}\mathcal{P}_{\boldsymbol{z}}^2\right) \right.$$
$$\times S_{i,\mathcal{P}_{\boldsymbol{x}}} S_{j,\mathcal{P}_{\boldsymbol{z}}} + \left(6 - \frac{2}{3}|\mathcal{P}_{\boldsymbol{z}}|^2\right) S_{i,\mathcal{P}_{\boldsymbol{x}}} S_{j,\mathcal{P}_{\boldsymbol{z}}^*} \right\rangle, \qquad (31)$$

where, again, the dependence on the lattice site $\boldsymbol{z}$ has been made explicit.

C. Normalization

We have seen that, for every pair of lattice sites $\boldsymbol{x}$ and $\boldsymbol{y}$, we end up with a linear system of equations for the couplings of the effective theory. Since on the lattice we have both translational and (discrete) rotational symmetry it is sufficient to consider different distances $d = |\boldsymbol{x} - \boldsymbol{y}|$ only. These serve as a label for our sets of equations which in a condensed matrix notation may be written as

$$M_d \boldsymbol{\lambda} = \boldsymbol{b}_d. \qquad (32)$$

If we assume a total of N unknown couplings collected into the vector $\boldsymbol{\lambda}$ we have, by construction of the SDEs, an $N \times N$ matrix M_d and an inhomogeneity $\boldsymbol{b}_d$, hence an independent system of equations, for each distance d. The off-diagonal entries of M_d and the vector $\boldsymbol{b}_d$ are typically complex but the couplings $\boldsymbol{\lambda}$ have to be real. We therefore distinguish between real and imaginary parts of (32) for different d and group them together into the equations

$$\begin{pmatrix} \text{Re } M_0 \\ \text{Im } M_0 \\ \text{Re } M_1 \\ \text{Im } M_1 \\ \vdots \\ \text{Im } M_{\lfloor N_s/2 \rfloor} \end{pmatrix} \boldsymbol{\lambda} = \begin{pmatrix} \text{Re } \boldsymbol{b}_0 \\ \text{Im } \boldsymbol{b}_0 \\ \text{Re } \boldsymbol{b}_1 \\ \text{Im } \boldsymbol{b}_1 \\ \vdots \\ \text{Im } \boldsymbol{b}_{\lfloor N_s/2 \rfloor} \end{pmatrix}. \tag{33}$$

This constitutes an overdetermined linear system of $2N \times (\lfloor N_s/2 \rfloor + 1)$ equations for the N unknown couplings $\boldsymbol{\lambda}$. In principle, this can be solved by standard least-square methods.

However, this procedure is hampered by a few technical pitfalls. Since the order parameter for the confinement-deconfinement transition is driven by the long-range behavior of the lattice system we have to take into account the fact that equations associated with different distances d enter (33) with different multiplicities. On a three-dimensional lattice this entails that an equation for distance $d > 0$ has multiplicity

$$m_d \equiv (2d + 1)^3 - (2d - 1)^3 \tag{34}$$

while equations for $d = 0$ only appear once. To account for this mismatch we reweight the coefficients of $\boldsymbol{b}_d$ and M_d (for $d > 0$) with a factor $\sqrt{m_d}$.

Another problem are the large condition numbers of the matrices. To cope with this we employ a simple form of normalization based on the diagonal elements of the matrix M_0. For the algebraic SDEs the diagonal entries $M_{0,ii}$ of M_0 dominate the linear system. For this reason we construct a new diagonal matrix N_0 from the $M_{0,ii}$ according to

$$N_0 \equiv \text{diag}(\text{Re}(M_{0,11})^{-1/2}, \ldots, \text{Re}(M_{0,NN})^{-1/2}). \tag{35}$$

By means of a similarity transformation with N_0 the real parts of the $M_{0,ii}$ may be transformed to unity. As a result (33) becomes

$$(N_0 M_d N_0)(N_0^{-1} \boldsymbol{\lambda}) \equiv (N_0 M_d N_0) \boldsymbol{\mu} = N_0 \boldsymbol{b}_d. \tag{36}$$

Typically, this new system of equations is better conditioned which increases the stability of the results.

In our numerical calculations we have both used the improvement (36) in condition numbers and the reweighting factors given by the square root of (34).

IV. NUMERICAL RESULTS

The IMC method basically amounts to solving the SDEs (26) or (31), the crux being the evaluation of the expectation values $\langle \ldots \rangle$ in the *microscopic* ensemble. In our case this is given by a sufficient number of $SU(3)$ Yang-Mills configurations generated by standard heat bath MC routines [35–37].

At this point it seems worthwhile to emphasize that we do *not* perform any decimation steps or renormalization group transformations when we determine the effective couplings. Our IMC procedure rather relates Yang-Mills configurations—which may (equivalently) be regarded as being distributed according to the *full* effective action—to configurations generated with *truncated* effective actions. Once the effective couplings are determined all effective observables (i.e. monomials or correlators of traced Polyakov loops) are computed from configurations that are properly thermalized with respect to the truncated effective actions. The error inherent in this method may be related to the problem of finding improved actions for the microscopic dynamics as discussed in [38]. As our method is designed to only describe the dynamics of a macroscopic variable, the Polyakov loop, we can and do not expect that any of our truncated distributions will exactly match the microscopic one. Had we forgotten a dominant coupling in a truncated effective action it would have led to large *systematic* deviations of our observables from their microscopically determined counterparts. In order to correctly match observables we checked explicitly that all our measurements were free from thermalization effects. For this purpose we monitored the lattice averaged Polyakov loop in Monte Carlo time and omitted the initial sweeps (up to 10% of the total number) for which the Polyakov-loop distribution still differed from its equilibrium shape.

In what follows we will consider three *ansätze*, one with five NN couplings and two more general ones which either contain NN terms in higher representations or additional NNN couplings. In a strong-coupling expansion (which is rationale for the κ-actions) both the five leading NN terms as well as the NNN ones would be of order β^{2N_t} while the extended NN ones would be $\mathcal{O}(\beta^{3N_t})$.

A. NN couplings

Before one determines the effective couplings corresponding to Yang-Mills it is prudent to check if the SDEs (26) and (31) derived above are consistent within the effective theories themselves. To test for that we have first simulated an effective theory with five fixed input couplings and tried to reproduce them via IMC. The associated configurations were created with a standard Metropolis algorithm since the nonlinear interaction terms of the effective action render heat bath methods unfeasible. In order to compensate for the well-known shortcomings of this rather basic approach we had to use up to 10^6 sweeps corresponding to 10^3 uncorrelated configurations.

In Table I we have listed the outcome of our testing procedure. One notes that the couplings $\lambda_{i,\text{IMC}}$ determined via IMC coincide with the chosen input couplings $\lambda_{i,\text{input}}$ to an accuracy of about 2%, both for the algebraic and geometrical SDEs, where the statistical errors were computed via a standard jackknife procedure. This tells us two things, first that our SDEs (26) and (31) are both correct and, second, that IMC works extremely well for the effective theories.
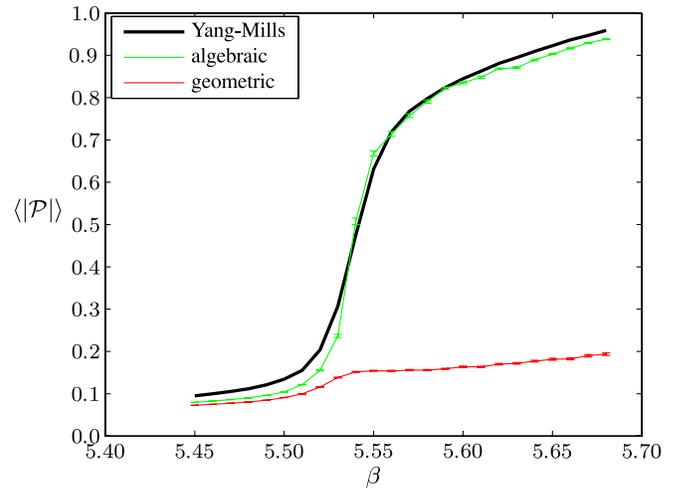
TABLE I. IMC consistency check for the NN λ-action including five couplings $\lambda_1, \ldots, \lambda_5$.

|	Algebraic		Geometrical	
i	$\lambda_{i,\text{input}}$	$\lambda_{i,\text{IMC}}$	$\lambda_{i,\text{input}}$	$\lambda_{i,\text{IMC}}$
1	-0.0100	$-0.0101(1)$	-0.0100	$-0.0101(1)$
2	0.0060	$0.0059(1)$	0.0060	$0.0060(1)$
3	-0.0050	$-0.0051(1)$	-0.0050	$-0.0051(1)$
4	0.0080	$0.0079(1)$	0.0080	$0.0080(1)$
5	-0.0060	$-0.0059(4)$	-0.0060	$-0.0060(2)$

Having thus gained confidence in the validity of our IMC approach and its implementation we can move on to apply it to our objective, namely, to determine effective actions reproducing Yang-Mills thermodynamics, in particular, the deconfinement phase transition. The first question we want to consider is whether the effective couplings λ_i viewed as functions of the Wilson coupling β are sensitive to the phase transition.

The answer turns out to be affirmative: Fig. 1 clearly shows a rather drastic change in the behavior of the couplings at a value of $\beta_\lambda \simeq 5.69$ for all λ_i, $i = 1, \ldots, 5$. Across the transition, i.e. in both phases the dominant coupling is the "fundamental" one, λ_1, followed by the octet couplings λ_3 and λ_5. The latter is actually a "potential" coupling in the sense of [24] as it multiplies the center symmetric single-site octet character χ_{11} (see Appendix A). The couplings λ_2 and λ_4 are clearly subdominant.

The natural observable to address is, of course, the Polyakov loop which serves as the order parameter of the first-order $SU(3)$ phase transition. In Fig. 2 we compare the effective and Yang-Mills Polyakov loops for a relatively small lattice of size $8^3 \times 3$ where the would-be disconti-

FIG. 2 (color online). Comparison between Yang-Mills and effective Polyakov loops for a lattice of size $8^3 \times 3$ and five NN couplings $\lambda_1, \ldots, \lambda_5$.

nuities (in infinite volume) of the transition are still fairly smooth. Somewhat surprisingly it is only the algebraic SDEs which reproduce the behavior of the Yang-Mills Polyakov loop reasonably well. The geometrical SDEs, on the other hand, fail to do so, at least in the region just above the transition point. This is a first hint that there is some inherent instability in the IMC procedure—in particular if the geometrical SDEs are used.

If we move on to larger lattices where the jump of the order parameter at the critical coupling becomes more pronounced one finds the behavior displayed in Fig. 3. Again, the algebraic SDEs work satisfactorily unlike the geometric ones for which, in particular, the sudden rise of the order parameter appears at a larger value of β, namely
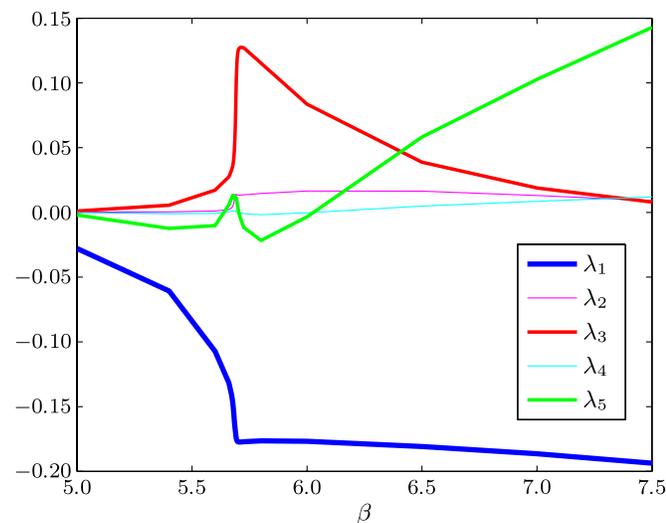
FIG. 1 (color online). Behavior of the couplings $\lambda_1, \ldots, \lambda_5$ (appearing in the NN λ-action) as a function of the Wilson coupling β. (IMC based on algebraic SDEs with $N_t = 4$.)
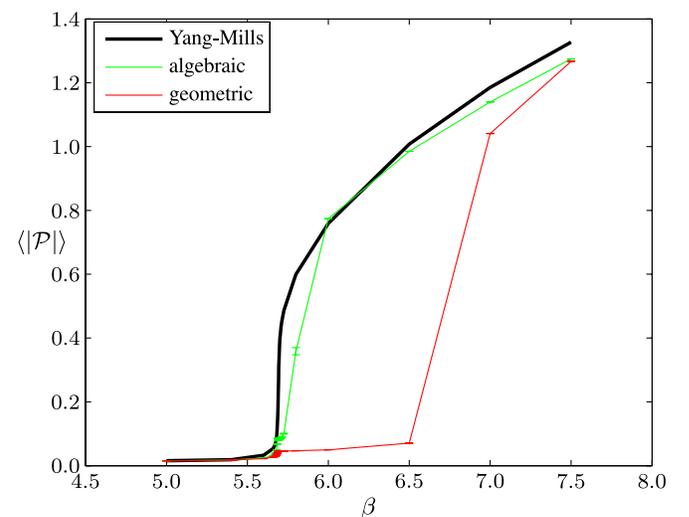
FIG. 3 (color online). Comparison between Yang-Mills and effective Polyakov loops for a lattice of size $16^3 \times 4$ and five NN couplings $\lambda_1, \ldots \lambda_5$.

$\beta_{\text{geo}} \simeq 6.5$. This is substantially larger than the critical coupling, $\beta_c \simeq 5.7$. Our explanation for this behavior is the fact that, due to the first-order nature of the transition, there are rather sharp phase boundaries in the space of coupling constants, λ_i. Hence, a tiny change in the couplings (presumably well within the IMC error bars) may easily have a large effect: by straying into the "wrong" phase the Polyakov loop will suddenly explode or collapse. This nonlinear effect is rather difficult to evade considering the unavoidable (if small) instabilities of the IMC procedure. As a result, as we inevitably increase these inaccuracies by adding more coupling we expect this fine-tuning problem to become enhanced even further. The following subsection will precisely address this topic.

B. NN and NNN couplings

There are (at least) two possibilities to generalize the NN λ-action of the previous subsection. One may either extend the NN terms to higher group representations or include interactions of larger range, say NNN.

The new NN terms we will add are of strong-coupling order β^{3N_t}, the additional NNN terms of order β^{2N_t}. As we are working at large β one cannot predict which ones are going to be more important. Rather, this will be one of the questions to be considered in what follows.

As before we have first tested the consistency of our SDEs. Table II shows once again that even for a total of the order of 10 couplings the method works well: IMC output reproduces input for the effective theory. The empty input entries in Table II correspond to vanishing couplings. For a few sample couplings we have checked that vanishing input correctly entails vanishing output as well.

TABLE II. IMC consistency check for the extended NN and NNN λ-actions including up to 11 couplings λ_i. (IMC based on algebraic SDEs.)

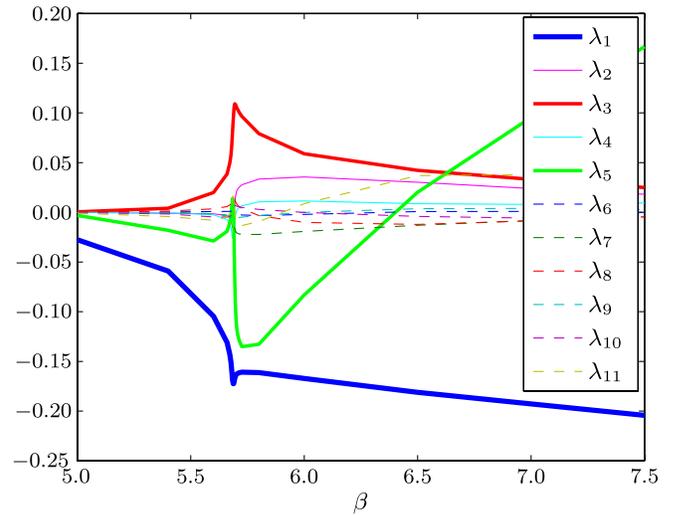|	Extended NN		NN + NNN	
i	$\lambda_{i,\text{input}}$	$\lambda_{i,\text{IMC}}$	$\lambda_{i,\text{input}}$	$\lambda_{i,\text{IMC}}$
1	-0.0050	$-0.0050(1)$	-0.0400	$-0.0400(1)$
2	0.0100	$0.0100(1)$	0.0100	$0.0099(1)$
3	-0.0150	$-0.0151(2)$	-0.0200	$-0.0201(1)$
4	0.0070	$0.0070(1)$	0.0300	$0.0300(1)$
5	-0.0080	$-0.0080(5)$	0.0050	$0.0052(3)$
6	0.0090	$0.0091(1)$		
7	0.0030	$0.0030(1)$		
8	-0.0030	$-0.0030(1)$		
9	0.0080	$0.0081(1)$		
10	-0.0060	$-0.0058(1)$		
11	0.0020	$0.0020(2)$		
12			-0.0020	$-0.0021(1)$
13			0.0060	$0.0060(1)$
14			-0.0030	$-0.0030(1)$
15			0.0040	$0.0039(1)$
16			-0.0070	$-0.0070(1)$

FIG. 4 (color online). Behavior of the couplings $\lambda_1, \ldots, \lambda_{11}$ (appearing in the extended NN λ-action) as a function of the Wilson coupling β. (IMC based on algebraic SDEs.)

To determine the behavior of the effective couplings λ_i, $i = 1, \ldots, 16$, as a function of the Wilson coupling β we have used a set of 4×10^6 configurations per β on a $16^3 \times 4$-lattice. This amounts to 5×10^4 (10^3) uncorrelated configurations far away from (close to) the phase transition. The IMC results are shown in Figs. 4 and 5 displaying the effective couplings as functions of β. Again we note that the fundamental and octet potential couplings (λ_1 and λ_5) dominate in size. More important from a principal point of view, however, is the observation that the behavior of coupling constants is very sensitive to the choice of operators. Let us compare, for instance, the coupling λ_3 in the two Figs. 4 and 5. For the extended NN *ansatz* (Fig. 4) it is
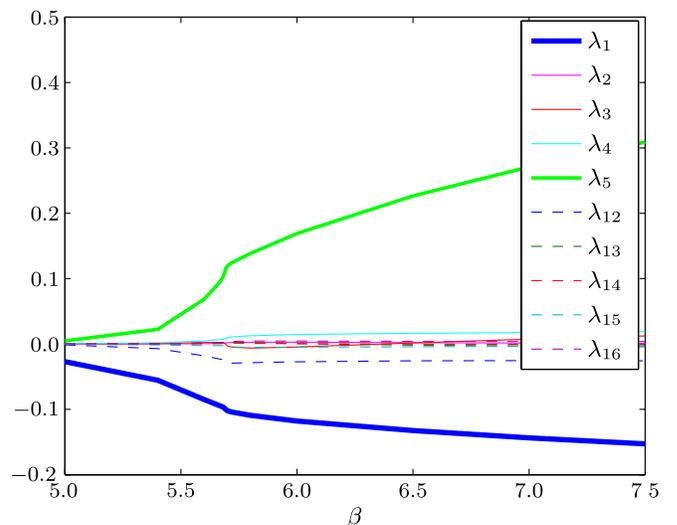

FIG. 5 (color online). Behavior of the couplings $\lambda_1, \ldots, \lambda_5$, $\lambda_{12}, \ldots, \lambda_{16}$ (appearing in the NN + NNN λ-action) as a function of the Wilson coupling β. (IMC based on algebraic SDEs.)
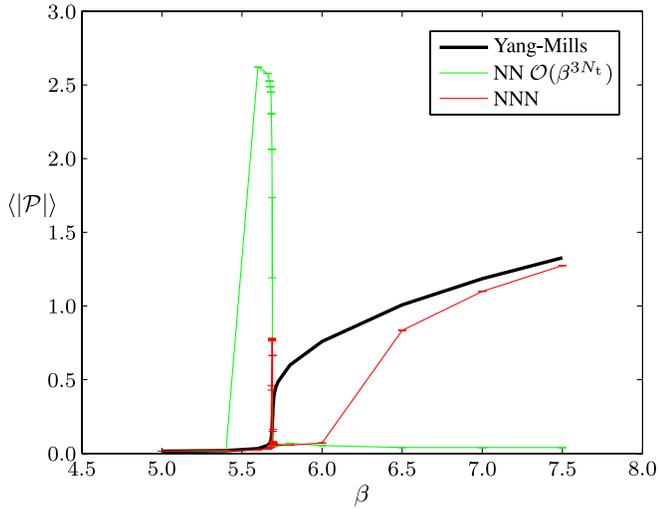
FIG. 6 (color online). Comparison between Yang-Mills and effective Polyakov loops for the extended NN action (couplings $\lambda_1, \ldots, \lambda_{11}$) and the NN + NNN action (couplings $\lambda_1, \ldots, \lambda_5$, $\lambda_{12}, \ldots, \lambda_{16}$) obtained from algebraic SDEs.

comparable in magnitude with λ_1 and λ_5 and behaves similarly as for the simple NN *ansatz* of Fig. 1. However, as soon as we include NNN operators its magnitude drops by 100% and its behavior changes drastically (Fig. 5). The latter is also true quite significantly for the octet coupling λ_5. This clearly signals an instability of the IMC methods, at least as far as the determination of the couplings is concerned.

Nevertheless, it might still be possible that largely different sets of couplings lead to more or less identical behavior of observables. Comparing the behavior of the Polyakov loop in the effective and Yang-Mills theories rules out this possibility. As Fig. 6 shows the Polyakov loop when calculated in the effective models is extremely sensitive to the choice of operators and the value of β around β_c. For both choices of SDEs the effective order parameter significantly overshoots the Yang-Mills one in a small β-range near β_c (see the spikes in Fig. 6). This means that in the space of effective couplings the phase boundary to the deconfined phase have slightly (and for a short range of β values) been crossed albeit with drastic effect due to the discontinuous behavior of the Polyakov loop. We conclude that the fine-tuning problem encountered in the previous subsection indeed becomes more severe if we include more operators (and hence increase the instabilities of the IMC procedure). For the given number of effective couplings (of order ten) we have not been able to get this problem under control.

V. SUMMARY AND OUTLOOK

In this paper we have applied the IMC method to study the finite-temperature phase transition of $SU(3)$ Yang-Mills theory. Crucial input were novel Schwinger-Dyson equations based on algebraic and geometrical properties of

the $SU(3)$ Haar measure. The resulting equations constitute overdetermined linear systems for the effective couplings λ_i which were solved numerically via least-square techniques. The method works well if the number of couplings is sufficiently small, say of the order of 5. However, already in this case one notes a fine-tuning problem as the behavior of the Polyakov loop depends in a very sensitive and non-linear way on the effective couplings.

This fact must be rooted in the discontinuities associated with the first-order character of the phase transition. There are at least three reasons in favor of this. First, the huge sensitivity is absent in $SU(2)$ [28] where the transition is of second order, hence continuous. As a result IMC works extremely well even if we include a total of 14 operators [27]. Second, the problem becomes more pronounced if we go to larger volumes whereupon the transition becomes increasingly sharper. Third, the sensitivity grows with the number of effective couplings included and hence with the error bars in the IMC procedure.

Indeed, if we increase the number of effective couplings and thus, inevitably, the instabilities in their IMC determination, the fine-tuning problem again becomes more severe as observed in Fig. 6. This holds to such an extent that we could no longer gain numerical control and hence could no longer reproduce the Yang-Mills behavior of the Polyakov loop in the vicinity of the critical Wilson coupling, $\beta = \beta_c$. We believe that an improvement on this situation will require nontrivial modifications of the IMC procedure like e.g. smoothening of the loop in order to avoid the unphysical spikes of Fig. 6. In addition, it would be interesting to check whether Creutz's microcanonical demon method [15] mentioned in the introduction yields better results.

We conclude, nevertheless, with the positive statement that the IMC method does work for the first-order $SU(3)$ transition as well if we allow for only a small number of terms in the effective Polyakov-loop actions.

ACKNOWLEDGMENTS

APPENDIX A: OPERATORS FOR THE λ-ACTIONS

In this paper we have used up to 16 different operators appearing in the λ-action (7):

$$S_1 = \sum_{\langle xy \rangle} (\chi_{10}(\mathcal{P}_x)\chi_{01}(\mathcal{P}_y) + \text{c.c.}), \qquad \text{(A1)}$$

$$S_2 = \sum_{\langle xy \rangle} (\chi_{20}(\mathcal{P}_x)\chi_{02}(\mathcal{P}_y) + \text{c.c.}), \qquad \text{(A2)}$$

$$S_3 = \sum_{\langle xy \rangle} \chi_{11}(\mathcal{P}_x)\chi_{11}(\mathcal{P}_y), \tag{A3}$$

$$S_4 = \sum_{\langle xy \rangle} (\chi_{10}(\mathcal{P}_x)\chi_{20}(\mathcal{P}_y) + \chi_{20}(\mathcal{P}_x)\chi_{10}(\mathcal{P}_y) + \text{c.c.}), \tag{A4}$$

$$S_5 = \sum_{x} \chi_{11}(\mathcal{P}_x), \tag{A5}$$

$$S_6 = \sum_{\langle xy \rangle} (\chi_{30}(\mathcal{P}_x)\chi_{03}(\mathcal{P}_y) + \text{c.c.}), \tag{A6}$$

$$S_7 = \sum_{\langle xy \rangle} (\chi_{21}(\mathcal{P}_x)\chi_{12}(\mathcal{P}_y) + \text{c.c.}), \tag{A7}$$

$$S_8 = \sum_{\langle xy \rangle} (\chi_{30}(\mathcal{P}_x)\chi_{11}(\mathcal{P}_y) + \chi_{11}(\mathcal{P}_x)\chi_{30}(\mathcal{P}_y) + \text{c.c.}), \tag{A8}$$

$$S_9 = \sum_{\langle xy \rangle} (\chi_{21}(\mathcal{P}_x)\chi_{20}(\mathcal{P}_y) + \chi_{20}(\mathcal{P}_x)\chi_{21}(\mathcal{P}_y) + \text{c.c.}), \tag{A9}$$

$$S_{10} = \sum_{\langle xy \rangle} (\chi_{21}(\mathcal{P}_x)\chi_{01}(\mathcal{P}_y) + \chi_{01}(\mathcal{P}_x)\chi_{21}(\mathcal{P}_y) + \text{c.c.}), \tag{A10}$$

$$S_{11} = \sum_{x} (\chi_{30}(\mathcal{P}_x) + \text{c.c.}), \tag{A11}$$

$$S_{12} = \sum_{[xz]} (\chi_{10}(\mathcal{P}_x)\chi_{01}(\mathcal{P}_z) + \text{c.c.}), \tag{A12}$$

$$S_{13} = \sum_{\langle xyz \rangle} (\chi_{10}(\mathcal{P}_x)\chi_{01}(\mathcal{P}_z) + \text{c.c.})\chi_{11}(\mathcal{P}_y), \tag{A13}$$

$$S_{14} = \sum_{\langle xyz \rangle} (\chi_{10}(\mathcal{P}_x)\chi_{02}(\mathcal{P}_y)\chi_{10}(\mathcal{P}_z) + \text{c.c.}), \tag{A14}$$

$$S_{15} = \sum_{\langle xyz \rangle} (\chi_{10}(\mathcal{P}_x)\chi_{10}(\mathcal{P}_y)\chi_{10}(\mathcal{P}_z) + \text{c.c.}), \tag{A15}$$

$$S_{16} = \sum_{(xy, vw)} (\chi_{10}(\mathcal{P}_x)\chi_{01}(\mathcal{P}_y) + \text{c.c.}) \cdot (\chi_{10}(\mathcal{P}_v)\chi_{01}(\mathcal{P}_w) + \text{c.c.}). \tag{A16}$$

The NN and NNN relationships are denoted in terms of brackets the meaning of which is explained in Fig. 7. Hence, the operators S_1 to S_{11} obviously describe (extended) NN interactions, while S_{12} to S_{16} are NNN terms. In a strong-coupling (small-β) expansion the terms $S_1, \ldots, S_5$ and $S_{12}, \ldots, S_{16}$ would be of $\mathcal{O}(\beta^{2N_t})$, the terms $S_6, \ldots, S_{11}$ of $\mathcal{O}(\beta^{3N_t})$ [31].
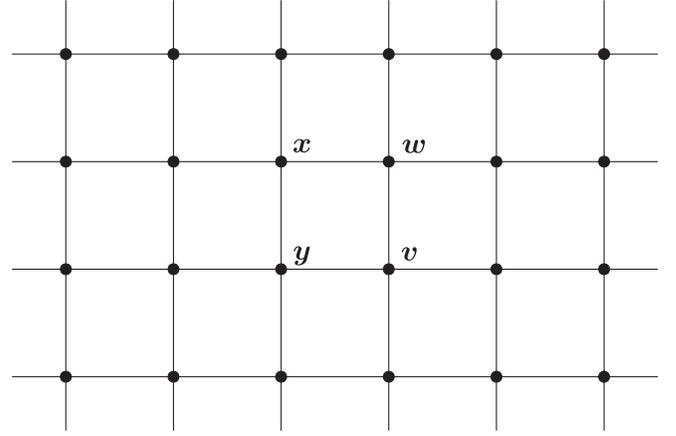

FIG. 7.   The neighboring relationships of the marked sites correspond to the bracket notations $[xv]$, $[yw]$, $\langle xyv \rangle$, $\langle yvw \rangle$, $\langle vwx \rangle$, $\langle wxy \rangle$, (xy, vw), and (xw, yv).

APPENDIX B: OPERATORS FOR THE κ-ACTIONS

If we extend the strong-coupling NN contributions to $\mathcal{O}(\beta^{3N_t})$ the effective action becomes a series of nine terms,

$$S_{\text{eff}} = \sum_{a=1}^{9} \kappa_a I_a, \tag{B1}$$

which is referred to as the extended NN-action (as is its λ-equivalent, see Appendix C below).

If we allow for NNN interactions (which, however, do not extend beyond single plaquettes) up to order $\mathcal{O}(\beta^{2N_t})$ we end up with the effective action

$$S_{\text{eff}} = \sum_{a \in \{1,2,3,4,10,11\}} \kappa_a I_a. \tag{B2}$$

This (and its λ-equivalent, see Appendix C below) is referred to as the NN + NNN action.

The resulting operators are given by

$$I_1 = \sum_{\langle xy \rangle} (\chi_{10}(\mathcal{P}_x)\chi_{01}(\mathcal{P}_y) + \text{c.c.}), \tag{B3}$$

$$I_2 = \sum_{\langle xy \rangle} (\chi_{20}(\mathcal{P}_x)\chi_{02}(\mathcal{P}_y) + \text{c.c.}), \tag{B4}$$

$$I_3 = \sum_{\langle xy \rangle} \chi_{11}(\mathcal{P}_x)\chi_{11}(\mathcal{P}_y), \tag{B5}$$

$$I_4 = \sum_{\langle xy \rangle} (\chi_{10}(\mathcal{P}_x)\chi_{01}(\mathcal{P}_y) + \text{c.c.})^2, \tag{B6}$$

$$I_5 = \sum_{\langle xy \rangle} (\chi_{30}(\mathcal{P}_x)\chi_{03}(\mathcal{P}_y) + \text{c.c.}), \tag{B7}$$

$$I_6 = \sum_{\langle xy \rangle} (\chi_{21}(\mathcal{P}_x)\chi_{12}(\mathcal{P}_y) + \text{c.c.}), \tag{B8}$$

$$I_7 = \sum_{\langle xy \rangle} (\chi_{10}(\mathcal{P}_x)\chi_{01}(\mathcal{P}_y) + \text{c.c.})$$
$$\cdot (\chi_{20}(\mathcal{P}_x)\chi_{02}(\mathcal{P}_y) + \text{c.c.}), \tag{B9}$$

$$I_8 = \sum_{\langle xy \rangle} (\chi_{10}(\mathcal{P}_x)\chi_{01}(\mathcal{P}_y) + \text{c.c.}) \cdot \chi_{11}(\mathcal{P}_x)\chi_{11}(\mathcal{P}_y),$$
$$\tag{B10}$$

$$I_9 = \sum_{\langle xy \rangle} (\chi_{10}(\mathcal{P}_x)\chi_{01}(\mathcal{P}_y) + \text{c.c.})^3, \tag{B11}$$

$$I_{10} = \sum_{\langle xyz \rangle} (\chi_{10}(\mathcal{P}_x)\chi_{01}(\mathcal{P}_y) + \text{c.c.})$$
$$\cdot (\chi_{10}(\mathcal{P}_y)\chi_{01}(\mathcal{P}_z) + \text{c.c.}), \tag{B12}$$

$$I_{11} = \sum_{(xy,vw)} (\chi_{10}(\mathcal{P}_x)\chi_{01}(\mathcal{P}_y) + \text{c.c.})$$
$$\cdot (\chi_{10}(\mathcal{P}_v)\chi_{01}(\mathcal{P}_w) + \text{c.c.}). \tag{B13}$$

APPENDIX C: LINEAR COUPLING RELATIONS

For the extended NN action (B1) the relation between the λ_i and the κ_a is

$$\begin{pmatrix} \lambda_1 \\ \lambda_2 \\ \lambda_3 \\ \lambda_4 \\ \lambda_5 \\ \lambda_6 \\ \lambda_7 \\ \lambda_8 \\ \lambda_9 \\ \lambda_{10} \\ \lambda_{11} \end{pmatrix} = \begin{pmatrix} 1 & 0 & 0 & 1 & 0 & 0 & 1 & 1 & 12 \\ 0 & 1 & 0 & 1 & 0 & 0 & 0 & 1 & 3 \\ 0 & 0 & 1 & 2 & 0 & 0 & 2 & 0 & 8 \\ 0 & 0 & 0 & 1 & 0 & 0 & 0 & 1 & 6 \\ 0 & 0 & 0 & 12 & 0 & 0 & 0 & 0 & 24 \\ 0 & 0 & 0 & 0 & 1 & 0 & 1 & 0 & 1 \\ 0 & 0 & 0 & 0 & 0 & 1 & 1 & 1 & 3 \\ 0 & 0 & 0 & 0 & 0 & 0 & 1 & 0 & 2 \\ 0 & 0 & 0 & 0 & 0 & 0 & 0 & 1 & 3 \\ 0 & 0 & 0 & 0 & 0 & 0 & 1 & 1 & 6 \\ 0 & 0 & 0 & 0 & 0 & 0 & 0 & 0 & 6 \end{pmatrix} \begin{pmatrix} \kappa_1 \\ \kappa_2 \\ \kappa_3 \\ \kappa_4 \\ \kappa_5 \\ \kappa_6 \\ \kappa_7 \\ \kappa_8 \\ \kappa_9 \end{pmatrix}. \tag{C1}$$

The analogous relation for the NN + NNN action (B2) is

$$\begin{pmatrix} \lambda_1 \\ \lambda_2 \\ \lambda_3 \\ \lambda_4 \\ \lambda_5 \\ \lambda_{12} \\ \lambda_{13} \\ \lambda_{14} \\ \lambda_{15} \\ \lambda_{16} \end{pmatrix} = \begin{pmatrix} 1 & 0 & 0 & 1 & 0 & 0 \\ 0 & 1 & 0 & 1 & 0 & 0 \\ 0 & 0 & 1 & 2 & 0 & 0 \\ 0 & 0 & 0 & 1 & 0 & 0 \\ 0 & 0 & 0 & 12 & 0 & 0 \\ 0 & 0 & 0 & 0 & 2 & 0 \\ 0 & 0 & 0 & 0 & 1 & 0 \\ 0 & 0 & 0 & 0 & 1 & 0 \\ 0 & 0 & 0 & 0 & 1 & 0 \\ 0 & 0 & 0 & 0 & 0 & 1 \end{pmatrix} \begin{pmatrix} \kappa_1 \\ \kappa_2 \\ \kappa_3 \\ \kappa_4 \\ \kappa_{10} \\ \kappa_{11} \end{pmatrix}. \tag{C2}$$

[1] A. M. Polyakov, Phys. Lett. B **72**, 477 (1978).
[2] L. Susskind, Phys. Rev. D **20**, 2610 (1979).
[3] K. Holland, P. Minkowski, M. Pepe, and U. J. Wiese, Nucl. Phys. **B668**, 207 (2003).
[4] J. Greensite, K. Langfeld, S. Olejnik, H. Reinhardt, and T. Tok, Phys. Rev. D **75**, 034501 (2007).
[5] L. G. Yaffe and B. Svetitsky, Phys. Rev. D **26**, 963 (1982).
[6] B. Svetitsky and L. G. Yaffe, Nucl. Phys. **B210**, 423 (1982).
[7] J. Polonyi and K. Szlachanyi, Phys. Lett. B **110**, 395 (1982).
[8] K. Holland, M. Pepe, and U. J. Wiese, Nucl. Phys. **B694**, 35 (2004).
[9] F. Green and F. Karsch, Nucl. Phys. **B238**, 297 (1984).
[10] M. Ogilvie, Phys. Rev. Lett. **52**, 1369 (1984).
[11] B. Svetitsky, Phys. Rep. **132**, 1 (1986).
[12] K. Holland and U.-J. Wiese, in *At the Frontier of Particle Physics—Handbook of QCD*, edited by M. Shifman (World Scientific, Singapore, 2001).
[13] M. Creutz, A. Gocksch, M. Ogilvie, and M. Okawa, Phys. Rev. Lett. **53**, 875 (1984).
[14] A. Gocksch and M. Ogilvie, Phys. Rev. Lett. **54**, 1772 (1985).
[15] M. Creutz, Phys. Rev. Lett. **50**, 1411 (1983).
[16] M. Falcioni, G. Martinelli, M. L. Paciello, G. Parisi, and B. Taglienti, Nucl. Phys. **B265**, 187 (1986).
[17] A. Gonzalez-Arroyo and M. Okawa, Phys. Rev. D **35**, 672 (1987).
[18] J. Deckert, S. Wansleben, and J. G. Zabolitzky, Phys. Rev. D **35**, 683 (1987).
[19] A. Gonzalez-Arroyo and M. Okawa, Phys. Rev. Lett. **58**, 2165 (1987).
[20] M. Fukugita, M. Okawa, and A. Ukawa, Phys. Rev. Lett. **63**, 1768 (1989).
[21] B. R. Moore and M. Ogilvie, Nucl. Phys. B, Proc. Suppl. **17**, 350 (1990).
[22] M. Hasenbusch, K. Pinn, and C. Wieczerkowski, Phys. Lett. B **338**, 308 (1994).
[23] B. Svetitsky and N. Weiss, Phys. Rev. D **56**, 5395 (1997).
[24] A. Dumitru, Y. Hatta, J. Lenaghan, K. Orginos, and R. D. Pisarski, Phys. Rev. D **70**, 034511 (2004).
[25] R. D. Pisarski, Phys. Rev. D **62**, 111501(R) (2000).
[26] R. D. Pisarski, Nucl. Phys. **A702**, 151 (2002).
[27] L. Dittmann, T. Heinzl, and A. Wipf, J. High Energy Phys. 06 (2004) 005.
[28] T. Heinzl, T. Kaestner, and A. Wipf, Phys. Rev. D **72**, 065005 (2005).
[29] C. Wozar, T. Kaestner, A. Wipf, T. Heinzl, and B. Pozsgay,

Phys. Rev. D **74**, 114501 (2006).

[30] A. Wipf, T. Kaestner, C. Wozar, and T. Heinzl, SIGMA **3**, 006 (2007).

[31] C. Wozar, diploma thesis, Friedrich-Schiller University, Jena, 2006 (in German).

[32] S. Uhlmann, R. Meinel, and A. Wipf, J. Phys. A **40**, 4367 (2007).

[33] M. Billo, M. Caselle, A. D'Adda, and S. Panzeri, Nucl. Phys. **B472**, 163 (1996).

[34] R. B. Potts, Proc. Cambridge Phil. Soc. **48**, 106 (1952).

[35] N. Cabibbo and E. Marinari, Phys. Lett. B **119**, 387 (1982).

[36] M. Creutz, Phys. Rev. D **21**, 2308 (1980).

[37] A. D. Kennedy and B. J. Pendleton, Phys. Lett. B **156**, 393 (1985).

[38] E. T. Tomboulis and A. Velytsky, Phys. Rev. D **75**, 076002 (2007).